EUROPEAN ORGANIZATION FOR NUCLEAR RESEARCH

CERN/EF 86-4
20 March 1986

A FAST ON-LINE TRIGGER FOR EVENTS WITH MULTIPLE HIGH TRANSVERSE MOMENTUM TRACKS

Athens[1]-Bari[2]-Birmingham[3]-CERN[4]-Paris (Collège de France)[5]-Paris (LPNHE)[6] Collaboration

W. Beusch[4], I.J. Bloodworth[3], F. Bourgeois[4], A.J. Burns[4], J.N. Carney[3], A. Corre[4], B. Ghidini[2], Y. Goldschmidt-Clermont[4], J. Kahane[5], J.B. Kinson[3], K. Knudson[4], V. Lenti[2], F. Navach[2], H. Pflumm[4], I.C. Print[3], E. Quercigh[4], M. Sené[6], R. Sené[5], H.R. Shaylor[3], M. Stassinaki[2], G. Vassiliadis[1], G. Zito[2] and R. Zitoun[6]

ABSTRACT

We present a fast (30 μs) on-line trigger that selects, from 300 GeV/c π^- interactions, events with three tracks of transverse momentum larger than 0.9 GeV/c. The essential features of this trigger are a fast read-out (300 ns per cluster) of wire chambers, situated on the chamber frame, and a digital computation of transverse momenta that can cope with multiple hits in the detectors of the trigger tracks. The digital computation is done with standard MBNIM modules.

Submitted to Nuclear Instruments and Methods in Physics Research

---

EF/2113F/WB/sb

1. INTRODUCTION

The study of elementary processes at the quark-gluon level necessitates experiments with high statistics on relatively low cross section processes. The Omega facility at CERN [1] is suitable for such experiments since it can handle instantaneous interaction rates of more than $10^6 s^{-1}$ (or an instantaneous luminosity of 0.04 $nb^{-1}s^{-1}$). At 300 GeV/c the events are very complex and each results in ~ 2000 bytes of data. Therefore, a very selective trigger must be used to achieve a manageable data rate. Furthermore, the trigger decision must be fast because the Omega readout electronics cannot accept a second event before it is either reset or read out. We report here on a trigger system with a logic constructed with MBNIM [2] modules that selects 1 in 2.10^4 interactions with an average dead time of 200 ns per interaction. A MBNIM trigger system based on particle selection by counter hodoscopes and cellular Cherenkov counters has been published previously [3]. The novel feature of the present trigger is the on-line computation of transverse momenta of several particles using, in particular, wire coordinates of trigger chambers.

The aim of the experiment is to study neutral resonance production at high transverse momentum (p_T) in the central rapidity region of $\pi^- p$ collisions at 300 GeV/c [4]. Such resonances may be directly produced in quark/gluon collisions or be a sign of the elusive gluonium. The two charged particles from the resonance decay are opposite in azimuth to one or more particle(s) balancing the transverse momentum. At the downstream end of the magnet these particles have been deflected by 6 Tm. For each track, the interaction of the beam with a thin target defines a vertex point; the three components of the momentum can be estimated from two further space points measured in the downstream region. However, in this experiment horizontal and vertical coordinates were measured separately. Therefore, the trigger system must be able to find high p_T tracks in the presence of many background combinations of points.

The experimental layout is described in sect. 2 where we also summarize the technique of the wire chamber readout used for triggering (more details of the system are given in the Appendix). In sect. 3 we present the logic of the triggering system. Results are shown in sect. 4 together with the conclusions.

2. EXPERIMENTAL APPARATUS

2.1 Spectrometer layout

Fig. 1 shows the layout of the Omega facility used for this experiment. Inside the magnetic field (central value B = 1.8 T) there are 15 Multiwire Proportional Chambers (MWPC) with a total of 37 planes. Two Drift Chambers (DC) outside the magnetic field are used to increase the precision on the track parameters and to find a first track segment for the pattern recognition [5]. Two large threshold Cherenkov counters (C1, C2) and three associated planes of counter hodoscopes (HY1, HY2, HY3) with vertical slabs are used for particle identificatiaon. In addition to this "standard" Omega equipment we used detectors specifically designed for this experiment:

(a) Two planes of scintillator hodoscopes (HZ1, HZ2) each consisting of four quadrants made of 15 horizontal slabs. The outline of these hodoscopes (fig. 2(a)) has been chosen such that no particle with $p_T < 0.6$ GeV/c can hit the sensitive region. This is illustrated by fig. 2(b) which shows the intersection with the plane of HZ1 of tracks with $p_T < 0.6$ GeV/c. The slabs of HZ1 and HZ2 were designed to cover the same solid angle, seen from the interaction vertex, in correlated pairs. Their width increases with |z| to keep the error on the dip angle λ constant at $\Delta\lambda/\lambda = 7\%$.

(b) Two modules of MWPC with two planes each (MY1, MY2 and MY3, MY4). These planes contain 4 mm pitch vertical wires between cathodes made of 12 μm mylar foil with graphite paint in three electrically insulated sections. These sections matched the shapes of the hodoscopes HZ1 and HZ2 and had a 20% voltage difference so that MY1 and MY3 were sensitive in the upper part while MY2 and MY4 recorded particles in the bottom part only.

2.2 Fast readout of the trigger chambers

The MWPC used in the trigger (MY1 to MY4) were read out in two ways:

(a) The normal readout of the Omega chambers with the functions of (digital) delay, time gating and multiplexing of wire coordinates performed by electronics on the chambers [6].

(b) The fast readout picks up the wire signals before the multiplexing of (a) and sends the coordinates of the wire cluster centroids to a receiver in the counting

room at a rate of 300 ns per coordinate. This receiver (FASTEN) stores the incoming data in a fast memory that can drive a MBNIM bus and into another memory read out by the CAMAC data way. The FASTEN module also signals the end of the data stream. After this time two nested do-loops going through all pairs of coordinates (e.g. MY1i, MY3j) can be started. More details about this new system are given in the Appendix.

3. TRIGGERING SYSTEM

Our triggering system has been designed for selecting a special high p_T track pattern, namely a positive and a negative particle (resonance decay product) opposite in azimuth to a third particle (fig. 3). All three tracks were required to have $p_T \geq 0.9$ GeV/c.

The desired trigger selectivity coupled with an acceptable dead time required the usual introduction of several trigger levels with increasing selectivity, decreasing rates and increasing dead time.

3.1 Zero level trigger

The purpose of the zero level trigger is to select events in which 3 or 4 quadrants of HZ1 have recorded at least one hit. Since the hodoscope signals are fed into strobed coincidence register (CHESTER) [7] at the front end a gate signal must be provided first. This signal was derived from an interaction trigger (beam signal AND veto of a downstream beam counter). With the signal cables available at the Omega this first sample and hold/reset operation had to last 130 ns. Within this time a multiplicity test on the four quadrants of HZ1 was performed(*) (zero level trigger); upon an unwanted result, all registers were reset; upon a positive result, the next trigger level was started.

3.2 First level trigger

At the first level the MBNIM system had to perform the following operations:

(a) Identify corresponding hits in HZ1 and HZ2, i.e. tracks pointing to the target. This was done in parallel for the four quadrants. The logic function

---

(*) Using discriminators LRS 4416B whose output drives the CHESTERs as well as coincidence registers LRS 4448.

$\sum_n \{HZ2\}_n$ AND $\{HZ2\,(HZ1)\}_n$

was performed with a bit assigner (BA) [7] for HZ2 (HZ1), and with an Arithmetic and Logic Unit (ALU) [7] for the OR ($\sum_n$) of the bit-by-bit ANDs.

(b) Verify that only one HZ1-HZ2 correspondence occurs per quadrant; more than one track would have lead to ambiguities at a later stage. The multiplicity on the ALU output (a) was checked with MUSIC [7] modules.

(c) Demand at least three quadrants fulfilling (a) and (b).

The conditions (a) to (c) corresponded to our particular pattern.

The frequency at this trigger level, which was reached after an additional 330 ns, was 1/1000 of the interaction rate. This type of trigger can be used more generally to select a given number of tracks with $p_T \geq 0.6$ GeV/c in a laboratory rapidity interval $2.5 < y_{lab} < 4.5$ and with an acceptance of 60% for an individual track.

At this level, the readout of the proportional and drift chambers was initialized. The built-in electronic delay would not have allowed much further delay, moreover the coordinates recorded in the MY chambers are needed at the second trigger level.

3.3 Second level trigger

At the second level the wire numbers recorded in the sensitive regions of MY1-MY3 and MY2-MY4 are combined in pairs in an attempt to form tracks. The parameters of these potential tracks are tested for a lower limit of p_T; in the experiment we used $p_T > p_T^* = 0.9$ GeV/c.

The y coordinates of a pair of MWPC (y_1 and y_2) are related to the track momentum p and to the azimuthal angle φ by the approximate linear functions

$$1/p = a_o + a_1 y_1 + a_2 y_2 ,$$

$$\sin\varphi = b_o + b_1 y_1 + b_2 y_2 .$$

The dip angle λ is given by

$$\tan \lambda = cz,$$

where z is determined by an element of HZ1. The coefficients a, b and c are dependent on the geometry and on the magnetic field; a mean position of the interaction vertex in the target is assumed. In order to minimize the on-line computations we did not use the obvious inequality

$$p_T \simeq p(\sin^2\varphi + \tan^2\lambda)^{1/2} \geq p_T^*, \qquad (1)$$

but an equivalent inequality

$$\sin^2\varphi + \tan^2\lambda - (1/p^2)\ p_T^{*2} \geq 0\ . \qquad (2)$$

The quantity $\tan^2\lambda$ was computed in one step from the single accepted correlation HZ1-HZ2 by a bit assigner used as a look-up table (top of fig. 4). The computation of the two other terms in several steps is shown schematically in fig. 4. The Random Access High Speed Memories (RAHM) [7] can be loaded to give any function (16 bits) of the input number (10 bits). If needed, multiplication or division by a power of 2 can be achieved by a "hardware shift", i.e. by displacing the data wires on the MBNIM bus. Binary addition or subtraction is performed by ALUs; the trigger decision, inequality (2) true or false, appears on the carry output of the last ALU. In fig. 4 one quadrant of HZ1-HZ2 appears combined with chamber coordinates that cover both upper quadrants. In fact, $\sin^2\varphi$ and p_T^{*2}/p^2 were added and/or subtracted to $\tan^2\lambda$ from the two quadrants in modules working in parallel. The validity of a $y_1 y_2 z$ combination was determined from the value of y_2. The full logic produced therefore four distinct yes/no decisions, corresponding to the four quadrants.

While at most one $\tan^2\lambda$ (z) per quadrant was present for an event, y_1 and y_2 had to run through all combinations of hits in the two planes. As described in sect. 2.2 the FASTEN modules can be interconnected to make a clock-driven double do-loop. The clock started ~ 8 μs after the first level trigger with the AND of the ready signals of the 4 FASTEN. The time between clock pulses was 300 ns. More than 30 combinations for each of the top and bottom halves, which were treated in parallel, could be tested for inequality (2) within 25 μs. We believe that the modular MBNIM system which can be cabled for a specific function is superior in this respect to any programmable device.

Since the trigger system uses a minimum of measured points (y_1, y_2, z) and the approximate eq. (1) to compute p_T, so we do not expect a high degree of accuracy on this quantity. The accuracy is, however, adequate as can be seen from fig. 5 where we have plotted p_T, determined by the trigger system versus p_T, determined by the full Omega spectrometer.

Requiring tracks in three quadrants exceeding the cut-off momentum $p_T^* = 0.9$ GeV/c reduced the trigger rate by a further factor 13 with respect to level 1. At this trigger rate and using MICE, a bit-slice PDP11 emulator [8] at the front end of the data acquisition computer, readout dead-time was not a limiting factor for the experiment.

4. RESULTS

The information from the hodoscopes HZ1 and HZ2 as well as the wire numbers of the triggering chambers were present on the MBNIM bus and also read out by the standard data acquisition. Detailed comparisons of the on-line trigger decision with its emulation on the computer were used as powerful tools for proper timing and debugging. Having achieved these, on-line and emulated triggers showed no discrepancies during the whole run.

In fig. 6(a) we show the scatter plot of all y_1-y_2 combinations (multiple entries) of events satisfying level 1. The domain of such combinations of true, reconstructed, tracks of this sample is shown in fig. 6(b). Fig. 6(c) shows the y_1-y_2 combinations selected by the level 2 trigger using level 1 data (as shown in fig. 6(a)) as input. These combinations are all within the allowed domain; therefore, the trigger has the required selectivity or, in other words, the system makes no errors in treating the stream of digital data.

In order to examine quantitatively the efficiency of the trigger we have analyzed the data off-line using the Omega pattern recognition and geometry program TRIDENT [5] to reconstruct the tracks. Such tracks are unambiguously associated with hits in the detectors used for triggering.

We first examine the reconstruction efficiency for events with level 1 triggers, then we use reconstructed level 1 events to test level 2.

From a sample of 480 000 level 1 triggers, 99700 (20.8%) events are found with three trigger tracks originating from the target and reconstructed with hits in the hodoscopes HZ1, HZ2 (which were used for triggering). Our events at 300 GeV have a large (~ 16) multiplicity of charged and neutral particles and the interaction rate of 1 μs^{-1} creates some background, mainly in the drift chambers (which have a drift time of 0.5 μs). Under these conditions the pattern recognition program [5] sometimes failed to find the triggering tracks. On the other hand, many hits in HZ1 and HZ2 were not produced by genuine trigger tracks but rather by secondary particles from interactions in the spectrometer of charged and neutral primaries. These losses and false triggers explain the relatively low (20.8%) yield of useful reconstructed events.

From the sample of 99 700 reconstructed level 1 events, we now retain those which have: (a) all three tracks with $p_T > 0.9$ GeV/c; and (b) all tracks recorded in MY1...MY4, i.e., good candidates for the level 2 trigger. This leaves a sample of 9843 events of good candidates. We have ordered the tracks of a triplet p_{T1}, p_{T2} and p_{T3} in decreasing order of their transverse momentum. Their p_T distribution is shown in fig. 7 as full lines. The level 2 trigger flag was also recorded for the reconstructed level 1 events. We find 12 600 such flagged events and their p_T distribution is shown as points in fig. 7. The limited accuracy of the on-line momentum measurement combined with the sharp rise of the spectrum towards low p_T explain the distribution of p_{T3}, the lowest p_T particle of the triplet and, in particular, the presence of events with $p_{T3} < 0.9$ GeV/c. Since p_{T2} is, by definition, bigger than p_{T3} there are less events below 0.9 GeV/c in the p_{T2} spectrum and again less in the p_{T1} spectrum. The level 2 sample has a component below 0.9 GeV/c and so is larger than the level 1 sample with a sharp cut (good candidates), the points then overtake the solid line in the p_{T1} spectrum. The spectra of all three particles in a triplet have identical shapes independent of the trigger level used, i.e. level 2 does not introduce a bias.

To quantify the efficiency of the level 2 trigger we have to compare 9843 events which are candidates for level 2 with 6469 events of this sample that were: (a) flagged by the level 2 trigger system and (b) had the lowest transverse momentum above 0.9 GeV/c. About 1900 events in the bin $0.9 < p_{T3} < 0.95$ GeV/c (fig. 7(c)) were lost by the momentum error of the level 2 at the edge of the cut; further losses are distributed uniformly over the p_{T3} spectrum. Within a few per cent the same residual losses (12%) are found when the level 2 algorithm is emulated off-line.

These losses are therefore explained by imperfections of the algorithm, e.g. cut-off at low momentum and at large angles, imprecise handling of z with a hodoscope of 15 elements only, etc.

In a 12 day run we have recorded 7×10^6 triggers yielding 10^6 events with 3 reconstructed tracks having $p_T > 0.9$ GeV/c each. One event represents a cross section of 0.4 p barn.

5 CONCLUSIONS

We have built and tested a fast multiparticle high p_T trigger using a MWPC's array which gives a good on-line measurement of p_T which is unbiased and has a reasonable efficiency. The analysis of an experiment which made use of such a trigger has confirmed our expectations.

APPENDIX

The FAST ReadOut system for wire chambers (FASTRO) differs from others in that wire signals are not brought to the counting room through long, numerous and expensive cables. Amplifiers, discriminators, digital delays and buffer registers are situated at one end of the chamber plane and they are connected to a double width CAMAC module, the FAST ENcoder (FASTEN) through a single 40-wire twisted pair cable.

The structure of FASTRO follows the organisation of the on-chamber electronics. Eight sense wires are connected for a minicard; sixteen minicards are plugged into a backplane board that carries power and control lines; a seventeenth socket is reserved for a card which, among other functions, carries a bus repeater.

A schematic of the FASTRO minicard is given in fig. 8. The amplifiers, discriminators and digital delays (for 8 wires) are common to FASTRO and to the slower serial read-out described in ref. [6]. The fast read-out section drives a 40 wire flat cable bus via a solder tail header connector. A bus segment can be connected to sixteen FASTRO minicards; bus segments can be daisy chained through the bus repeaters. The first bus segment of a MWPC plane is interfaced to the FASTEN module in order to allow for data transmission over long distances (typically 30 m).

To summarize, the on-chamber electronics involves three different minicards:

(a) the 8-channel FASTRO card,
(b) the bus repeater circuit (1 per 16 FASTRO), and
(c) the interface card (1 per plane).

For each first level trigger all digital delay sections of an MWPC plane are scanned. Wires with a signal within the gate time set flags into the buffer registors on the minicards. These registers, if they contain at least one hit from the corresponding eight wires, are sequentially read by means of:

(a) two fully handshaked control lines, and

(b) a daisy chained OR of the set bits, inhibiting all but the last minicard that contains information.

It can be seen that the readout speed is limited by the propagation time of the OR signals in the daisy chain. A bus segment OR (OR_{16} in fig. 8) has therefore been added that is daisy chained via the bus repeaters and that allows for a fast look-ahead for the next group of 16 minicards containing a hit.

The data format is straightforward and gives:

(a) the bit pattern in the least significant byte and,

(b) the minicard geographical position in the upper byte.

Hit bit patterns can be read every 300 ns for a 1 K channel system and cluster centroids are encoded by the FASTEN module without time overheads.

Coordinates are stored:

(a) into a 40-word deep FIFO buffer for later readout via the CAMAC dataway and

(b) into a fast memory driving an MBNIM port [2].

Front panel miniature coaxial sockets allow for the sequential scan of the fast memory. On-board switches are used to select the scanning direction and to define two acceptance windows. Thus, the FASTEN modules associated with two or more trigger planes can be easily wired to allow for nested loops.

The system is mostly built with low power Shottky TTL integrated circuits and is very reliable.

REFERENCES

[1] Omega Prime, compiled by W. Beusch, Technical Note, CERN/SPSC 77-10, SPSC/T17 (1977).

[2] A. Beer et al., Nuclear Instr. and Meth. 160 (1979) 217.

[3] T. Armstrong et al., WA60 trigger, Nuclear Instr. and Meth. 175 (1980) 543.

[4] Search for direct production of gluonium states in High p_T π^-N collisions at 350 GeV/c, WA77 Proposal, CERN/SPSC 82-62, SPSC P181 (1982).

[5] J.C. Lassalle et al., Nucl. Instr. and Meth. 176 (1980) 371.

[6] A. Beer et al., A pulse width modulation circuit for the remote readout of very long shift registers, Yellow Report CERN 78-14 (1978).

[7] F. Bourgeois, MBNIM User Guide, EF Division, January 1984, Edition 3.

[8] J.P. Dufey and S. Vascotto, CERN Mini and Micro Computer Newsletter No. 1, October 1983, p. 45.

FIGURE CAPTIONS

Fig. 1 Layout of the Omega system. The elements used for the trigger are: the counter hoodscopes with horizontal elements HZ1 and HZ2, the proportional chambers MY1 to MY4 with sensitive regions matched to the hodoscopes.

Fig. 2 (a) Outline drawing of hodoscope HZ2.

(b) Intersection with the plane of HZ2 of tracks with $p_T < 0.6$ GeV/c.

Fig. 3 Artist's view of an event. The tracks shown have been reconstructed from the data of the Omega system and extrapolated into the trigger detectors. The free triggering tracks are labelled $\pi 1$, $\pi 2$, $\pi 3$ and the elements of HZ1 and HZ2, hit by these tracks, are indicated.

Fig. 4 Schematic of second-level trigger. BA: bit assigner, RAHM: Random Access High speed Memory, +, (-) Arithmetic and Logic Unit (ALU) in addition (subtraction) mode.

Fig. 5 Scatter plot of p_T measured by the trigger system versus momentum measured by the Omega spectrometer.

Fig. 6 (a) scatter plot of all y_1-y_2 combinations (multiple entries) of events satisfying level 1.

(b) y_1-y_2 combinations of (a) associated to tracks.

(c) y_1-y_2 combinations selected by level 2.

Fig. 7 Transverse momentum distribution of the three trigger tracks (p_{T1}, p_{T2}, p_{T3}) ordered with decreasing momentum. Full lines: spectrum determined off-line from level 1 events; dots: spectrum of events satisfying the on-line trigger. The units of the ordinates are events/0.05 $(GeV/c)^2$.

Fig. 8 Schematic of the 8-channel FASTRO minicard. Wire signals are continually recorded in the n-bit electronic delay which is stopped whenever there is a level 1 trigger. The relevant data bits are then a fixed p locations from the input. A shift by (n-p) locations brings the data towards the output and hence sets the three output registers.

FIGURE CAPTIONS (Cont'd)

The serial out shift register is used for the slow readout of the data whereas the parallel out register displays the bit pattern on the FASTRO bus segment under control of the OR_n, Acknowledge and Data Ready signals. The OR16 line is used to speed up the slow propagation of the OR_n/OR_{n-1} signals (daisy chained).

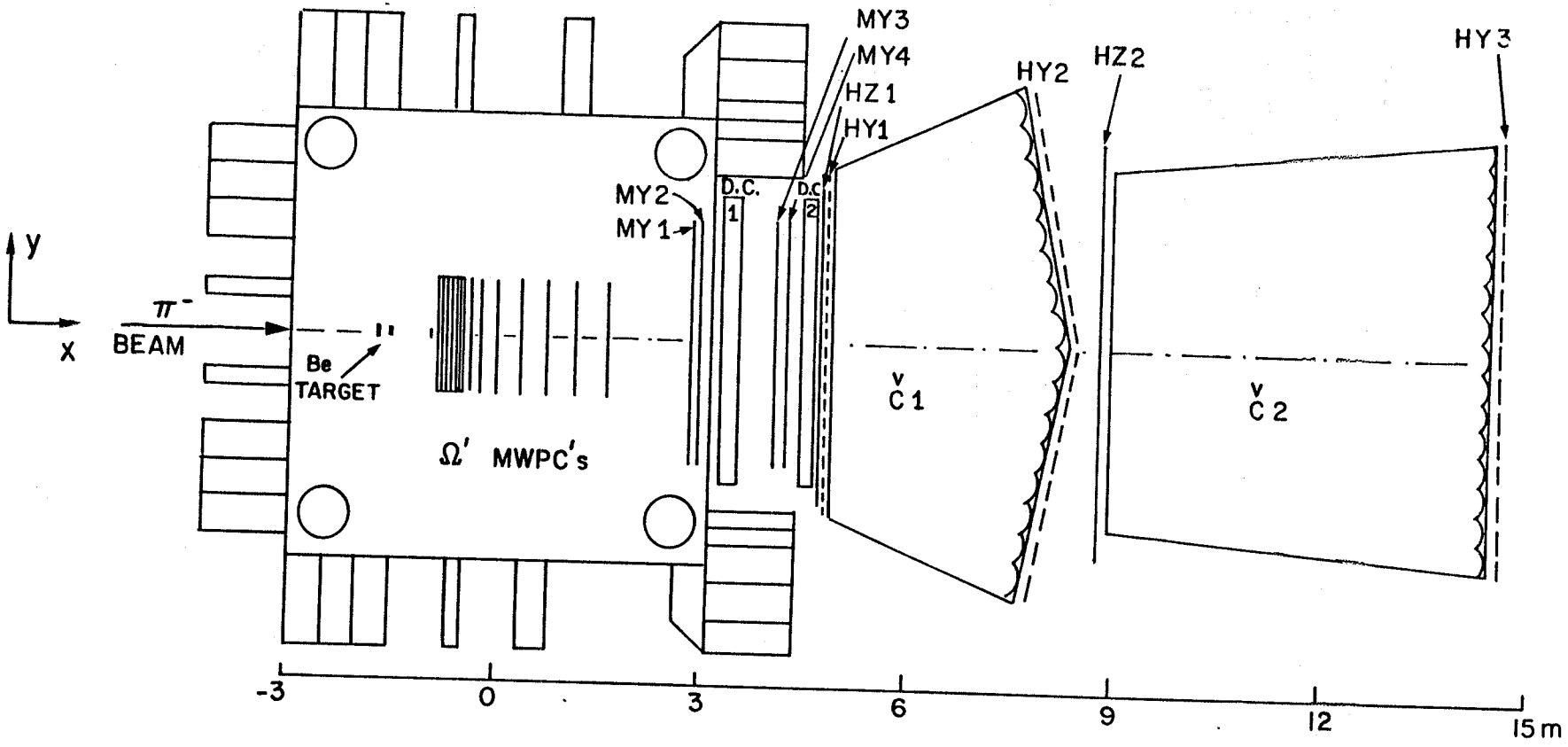
MY3
MY4
HZ1
HY1
HY2
HZ2
HY3
MY2
MY1
D.C. 1
D.C. 2
y
x
π⁻
BEAM
Be
TARGET
Ω' MWPC's
v C1
v C2
-3
0
3
6
9
12
15 m

Fig. 1

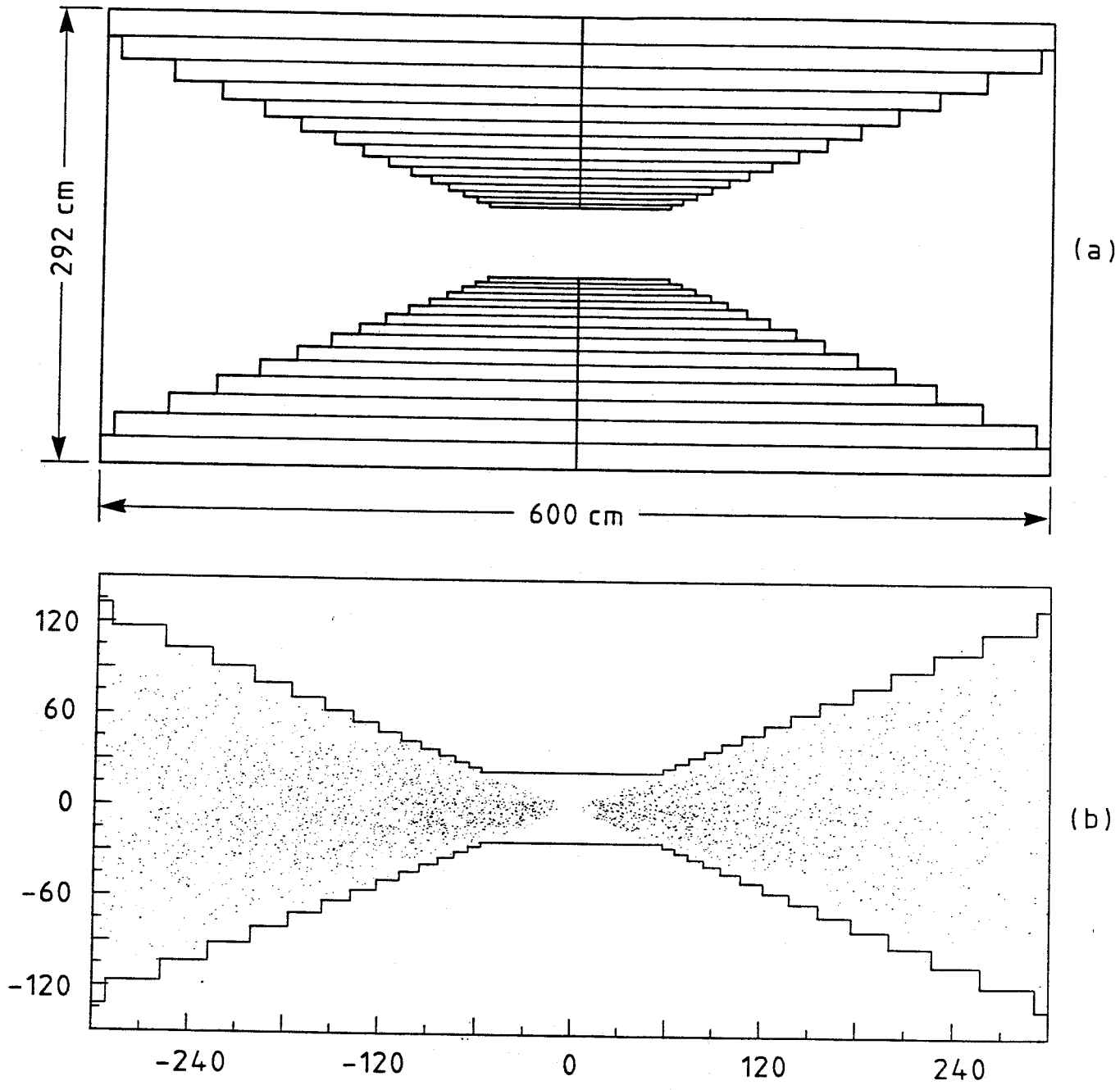

Fig. 2

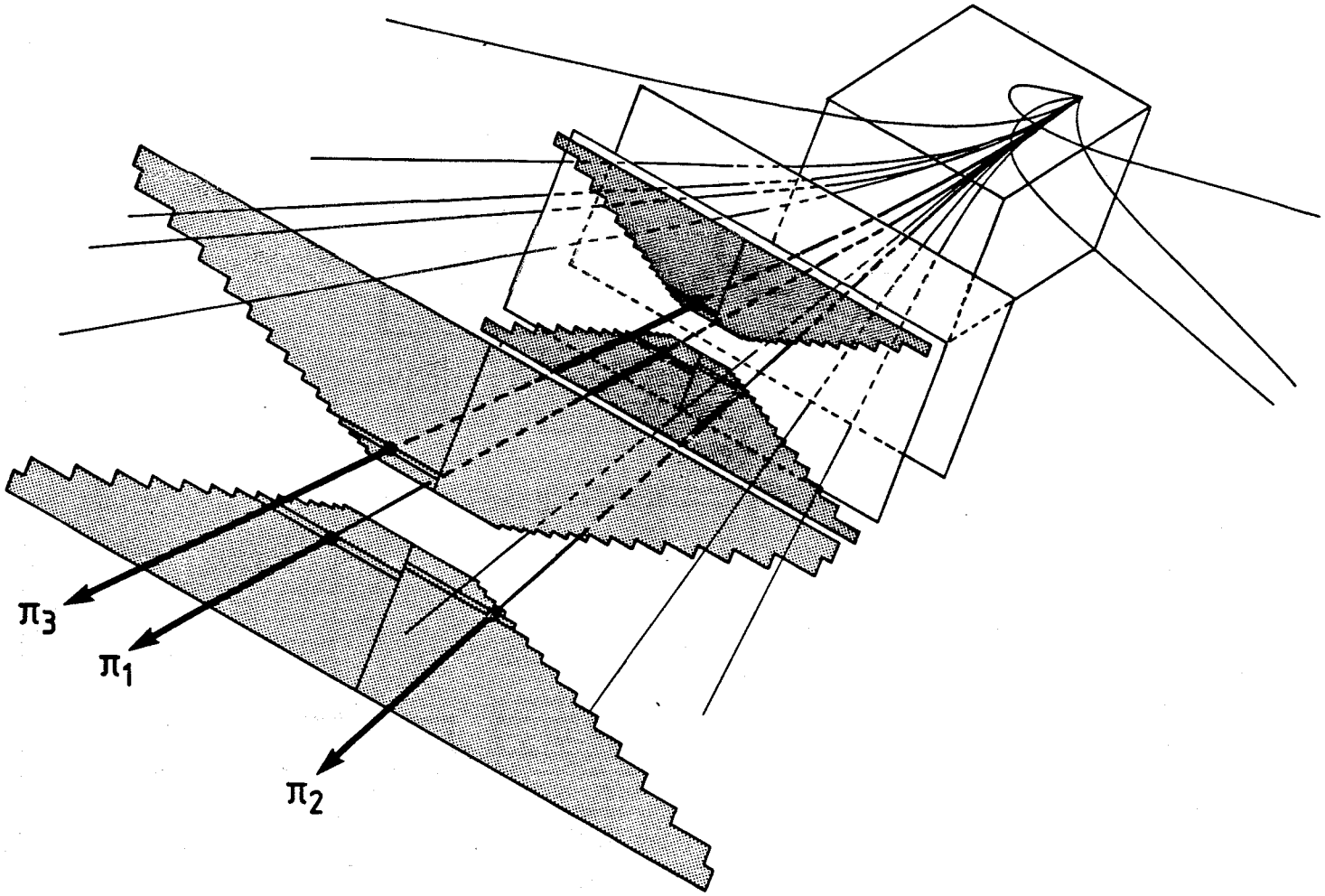

Fig. 3

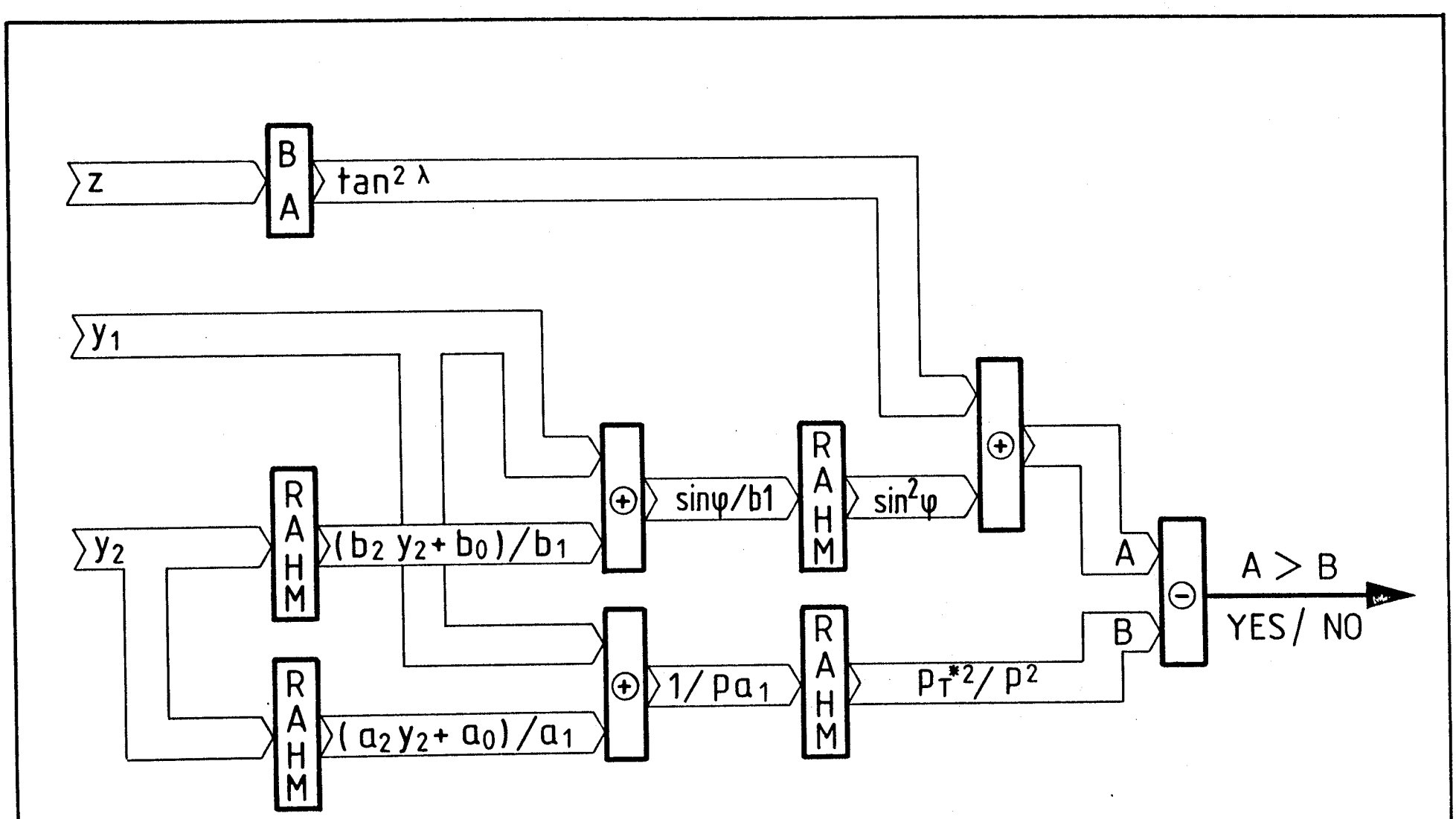
z
B
A
tan² λ
y1
y2
RAHM
(b2 y2 + b0)/b1
sinφ/b1
RAHM
sin²φ
A
A > B
YES/ NO
B
RAHM
(a2 y2 + a0)/a1
1/ Pa1
RAHM
PT*2/ P2

figure 4

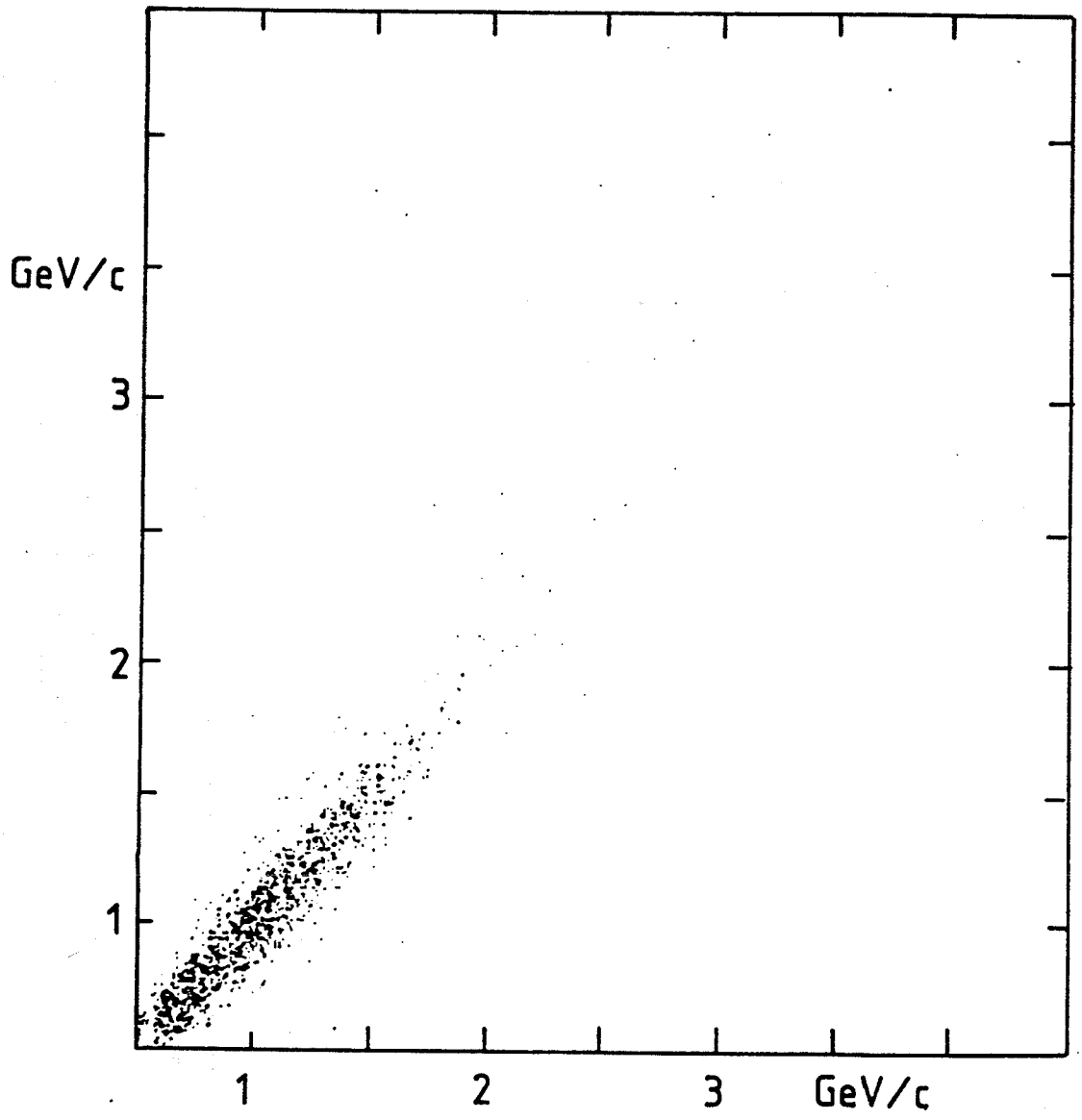

Fig. 5

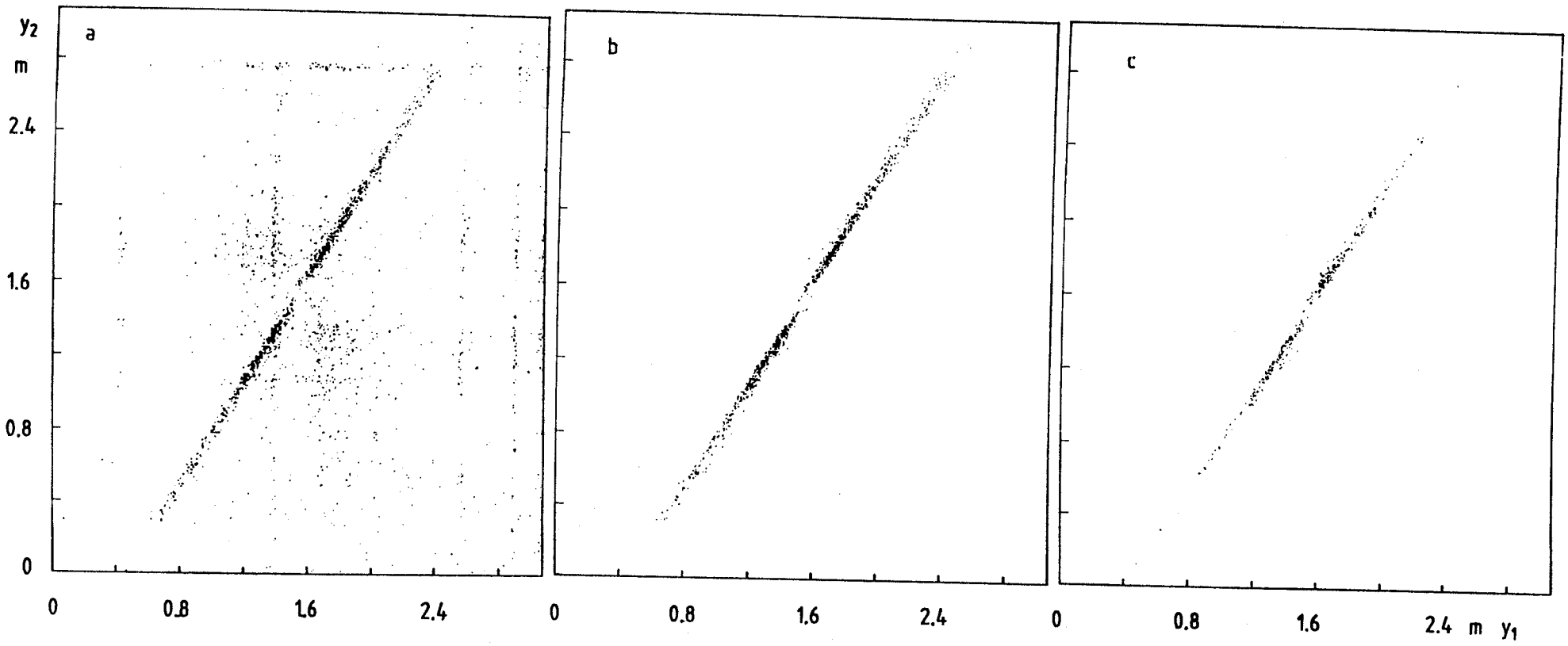

Fig. 6

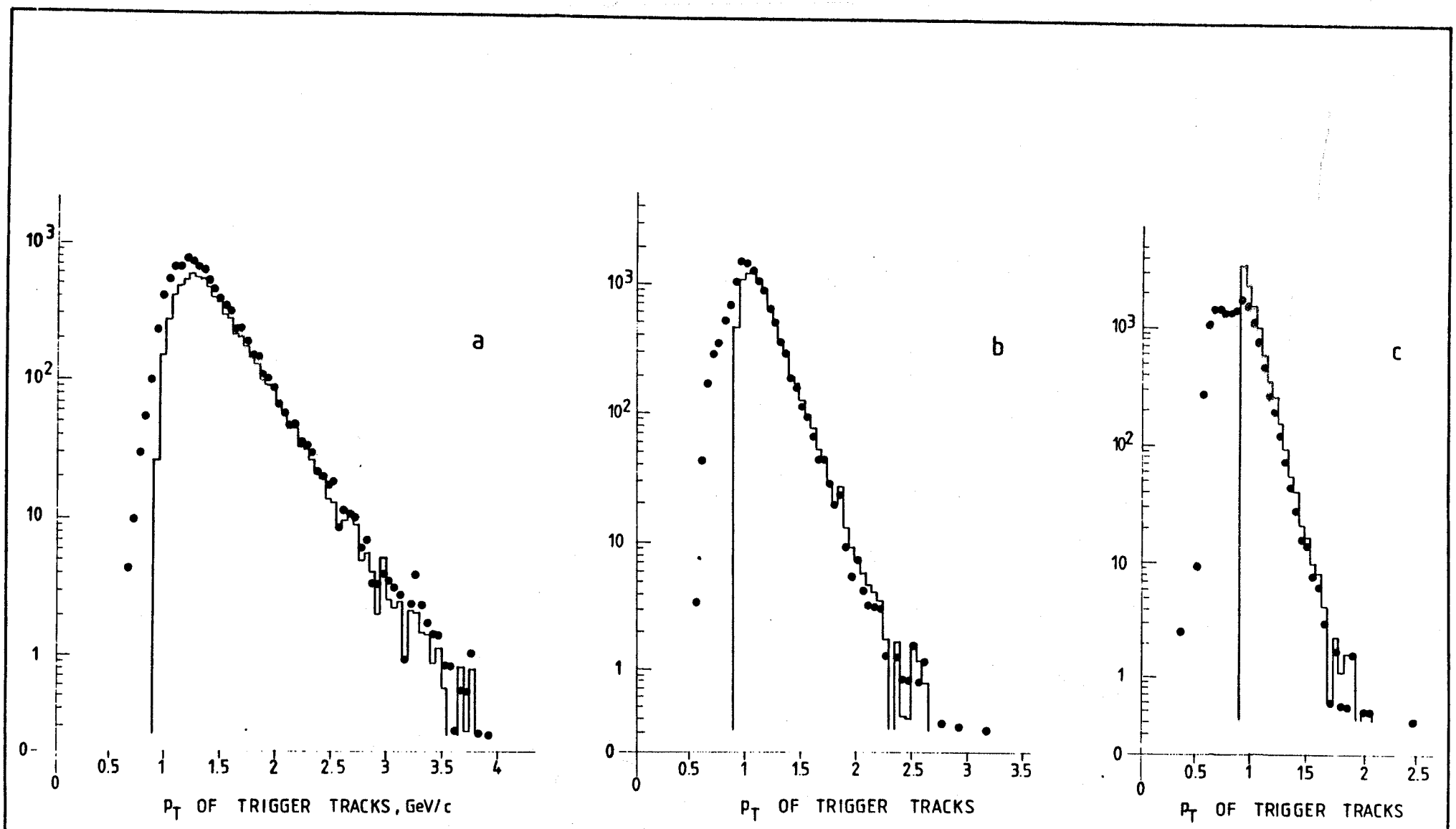
a
b
c
10^3
10^2
10
1
0
0.5
1
1.5
2
2.5
3
3.5
4
P_T OF TRIGGER TRACKS, GeV/c
P_T OF TRIGGER TRACKS

Fig. 7

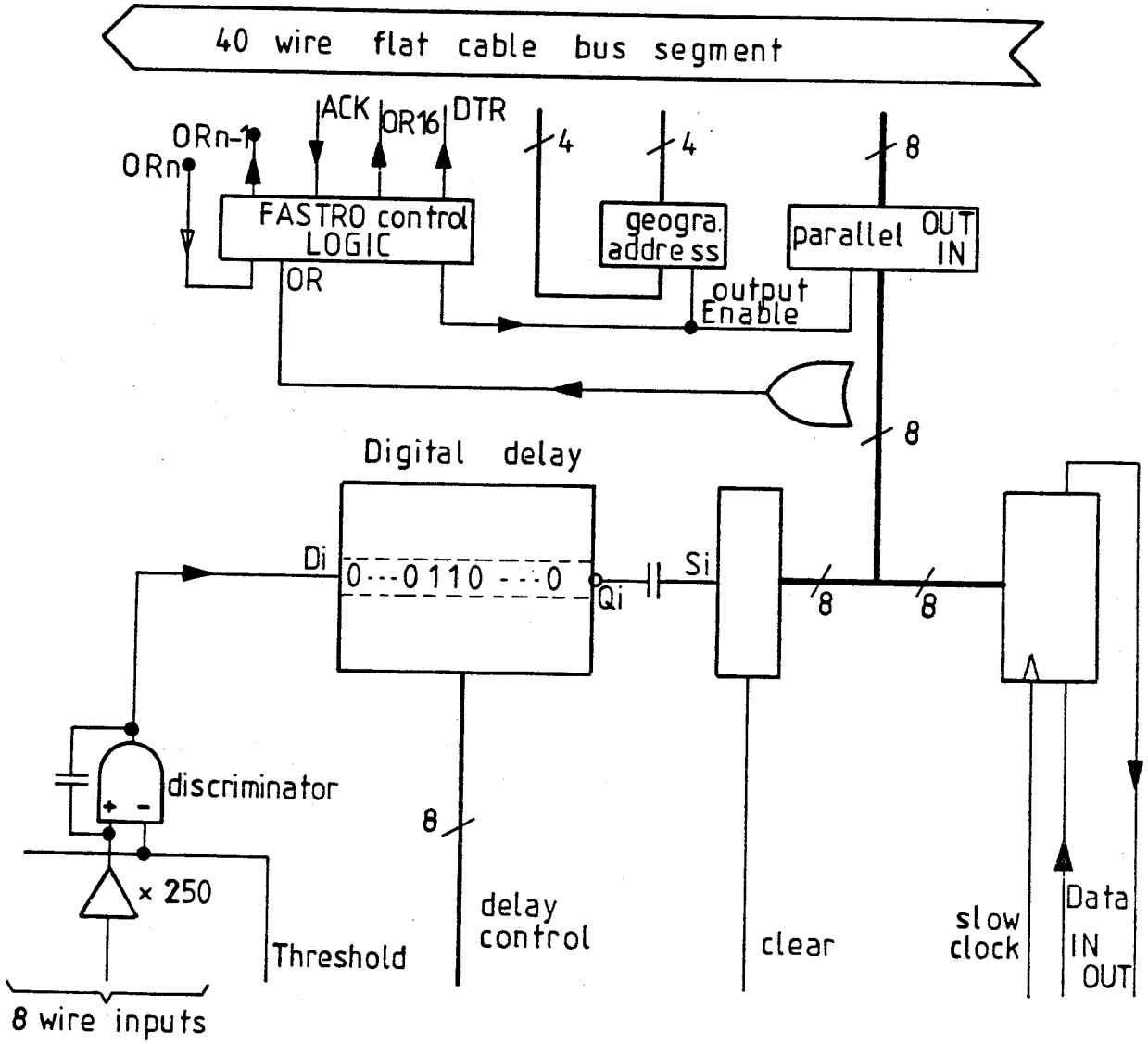

PC BOARD BACKPLANE

figure 8